Environmental Modelling & Software 18 (2003) 81–96

Environmental Modelling & Software

www.elsevier.com/locate/envsoft

WindStation—a software for the simulation of atmospheric flows over complex topography

A.M.G. Lopes

ADAI, Departamento de Engenharia Mecânica, Universidade de Coimbra, 3030 Coimbra, Portugal

Received 27 April 2001; received in revised form 19 October 2001; accepted 21 December 2001

Abstract

The present paper describes a software system aimed at the simulation of the wind field over complex topography. Two different models are implemented. Both these models predict wind speed and direction based on local measurements made with meteo stations. The whole system was developed under a graphical interface, aiming at a better ease of use and output readability. This paper describes the mathematical models employed and provides an overview of the graphical interface. Simulation results are compared with experimental data for an isolated hill and two situations of complex topography.

Keywords: Wind field; Kinematic models; Navier Stokes solver; Graphical User Interface

1. Introduction

The prediction of wind behaviour over complex topography is a valuable tool in areas such as the assessment of the wind energy potential of a given region, smoke and pollutant dispersal studies or even the prediction of forest fires' behaviour. The data supplied by meteo stations are punctual and thus, cannot be used directly for these applications, due to their inherently poor spatial description. This leads to the need of tools capable of predicting the wind at any location, taking as input, measurements performed by meteo stations. Several investigators have been working in this area, mainly after 1975. Jackson and Hunt presented, in 1975, in a pioneer work, an analytical model for the computation of the wind flow over two-dimensional smooth hills. This model was later modified by Taylor et al. (1983), to cope with three-dimensional hills. One of the main limitations of this model was its inherent restriction to smooth hills, where flow separation would not be expected. More sophisticated models appeared later, based on the algorithm SIMPLE proposed by Patankar (1980).

Non-linear models that solve the Navier-Stokes equations are capable of a more correct simulation of the wind field as a natural result of the incorporation of the most relevant physical phenomena into the simulation. Still, the weak point of these models lies in the turbulence modelling, where the available methods are not able to simulate completely the physics of the flow. In spite of this limitation, these models may provide, for some situations, good results and are also able to predict recirculation regions and effects of thermal stratification. Most models are based on the algorithm SIMPLE. Raithby and Stubley (1987) applied the SIMPLE method to a terrain-following co-ordinate system, along with a k-ϵ turbulence model, to simulate the wind flow over the Askervein hill. Askervein hill was the object of an extensive wind measurement program with the goal of providing benchmark data for validation purposes. Alm and Nygaard (1995) applied the Phoenics code to complex terrain, with good results. Uchida and Ohya (1999) presented a study on the influence of grid characteristics on the simulation of unsteady flows over complex terrain.

Mass-consistent models (also known as kinematic models) do not solve for momentum conservation. Their approach is simply to reach a divergence-free velocity field, starting with an initial solution obtained by interpolating the punctual meteo stations readings into all the grid points. The model NUATMOS (Ross et al., 1988), to be described later in this paper, follows this methodology, as well as the model by Szulényiová (1992).

The models presented previously are diagnostic mod-

1364-8152/02/$ - see front matter
PII: S1364-8152(02)00024-5

els, in the sense that they are aimed at the prediction of a steady state situation, corresponding to the time instant at which input data is supplied. Prognostic models follow a different approach, since they can predict the time evolution of the different variables, taking into account the diurnal cycle. These models, like MEMO (Flassak and Moussiopoulos, 1988), are aimed to predictions at larger scales and may be a good source of input data for more refined predictions.

The present work describes WindStation, an integrated system that incorporates CANYON, a Navier-Stokes solver (Lopes et al., 1995) and the kinematic model NUATMOS (Ross et al., 1988), within the graphical interface of the commercial CAD software Microstation, from Bentley Company. WindStation takes advantage of Microstation graphical environment and developing tools for designing user interface Dialog Boxes for data input and post-processing visualisation methods. The interfacing software was written in MDL, a Microstation specific C language, while the wind models, originally written in Fortran, run as external programs in a DOS window.

2. The mathematical models

2.1. Wind model NUATMOS

The model NUATMOS (Ross et al., 1988) is a mass-conservative model. It requires, as input data, the values of wind velocity and direction at a given number of punctual locations. The observations at the meteo stations are used as a basis for the construction of a first guess at every point of the three-dimensional domain, obtained by interpolation. Then, this initial guessed velocity field is adjusted following a method of variational analysis, under the restricting condition that, at every grid point, velocity magnitude and direction should undergo the least possible change. Controlling the amount of flexibility that is allowed for the vertical component of the velocity is the method employed for accounting for atmospheric stability.

Since NUATMOS does not solve for momentum conservation, the computational effort to run the model is very modest. A run for 100×100×20 grid points takes typically less than a minute to complete in a Pentium III personal computer. Nevertheless, due to its linear character, the non-linear phenomena associated with the flow over steeper topography, such as the occurrence of recirculation regions, cannot be predicted. Consequently, the results obtained by this model are more reliable for smooth topography, and the accuracy of the predictions is better over the up-stream side of the slopes. Despite these limitations, the solutions obtained with this model seem quite realistic in terms of interaction of the general wind with the local topography.

One of the characteristics of NUATMOS which is inherent to its solution approach, is the fact that the obtained solution does not, in general, satisfy the input data (wind speed and direction at the meteo stations location). WindStation incorporates a correction mechanism in which, after each NUATMOS run, the input is modified the proper amount in terms of wind speed and direction, so that the final solution will satisfy the input data. This is an iterative process, for which four iterations (NUATMOS runs) are generally enough to get a solution within 5% of the input data values. The mathematical formulation for the input correction, applied to each velocity component is the following:

$$x_2 = x_1 + 0.8(y_r - y_1) \tag{1}$$

where

x_2=new input value at the present iteration
x_1=input value at the previous iteration
y_r=reference value, i.e., reading at the meteo station
y_1=computed value at the meteo station, in the previous iteration.

The *0.8* factor was found by trial and error as a compromise between convergence rate and numerical stability.

2.2. Wind model CANYON

CANYON is a 3D Navier-Stokes solver written for a 3D generalised coordinate system (Lopes et al., 1995). The original Navier-Stokes equations, in their steady state formulation, are transformed into the generalised coordinate system through application of the chain rule and cast in the strong law conservation form, as follows:

$$\frac{\partial}{\partial \xi_j}(J\rho U_j u_i) = \frac{\partial}{\partial \xi_m}\mu_{eff} J\left[g^{mn}\frac{\partial u_i}{\partial \xi_n} + \frac{\partial \xi_m}{\partial x_j}\frac{\partial \xi_n}{\partial x_i}\frac{\partial u_j}{\partial \xi_n} - \frac{2}{3}\frac{\partial \xi_m}{\partial x_i}\frac{\partial \xi_n}{\partial x_j}\frac{\partial u_j}{\partial \xi_n}\right] - J\frac{\partial \xi_j}{\partial x_i}\frac{\partial P}{\partial \xi_j} - \frac{2}{3}J\left(\frac{\partial \xi_j}{\partial x_i}\frac{\partial(\rho k)}{\partial \xi_j}\right) \tag{2}$$

where u_i is a generic Cartesian velocity component, x_i and ξ_i are the generic Cartesian and computational coordinates, respectively, j is the summation index, U_i is a generic contravariant velocity component, the terms g^{mn} are contravariant metric relations, μ_{eff} is the effective viscosity and k is the turbulence kinetic energy.

The continuity requirement is expressed by the mass conservation equation, which generalized form is as follows:

$$\frac{\partial}{\partial \xi_i}(\rho J U_i) = 0 \tag{3}$$

A control volume approach is adopted for the integration of the transport equations. The SIMPLEC algorithm (Van Doormaal and Raithby, 1984) is employed as a means for the segregated solution of the primitive Cartesian velocity components (u, v, w) and pressure. Turbulence effects upon the mean flow field are modelled with recourse to the standard k-ε turbulence model (Launder and Spalding, 1974), whose equations are presented below.

$$\frac{\partial}{\partial x_i}(\rho u_i k) = \frac{\partial}{\partial x_i}\left[\left(\mu + \frac{\mu_t}{\sigma_k}\right)\frac{\partial k}{\partial x_i}\right] + P_1 - \rho\varepsilon \tag{4}$$

$$\frac{\partial}{\partial x_i}(\rho u_i \varepsilon) = \frac{\partial}{\partial x_i}\left[\left(\mu + \frac{\mu_t}{\sigma_\varepsilon}\right)\frac{\partial \varepsilon}{\partial x_i}\right] + \frac{\varepsilon}{k}(C_1 P_1 - C_2\rho\varepsilon) \tag{5}$$

$$P_1 = -\rho\overline{u_i' u_j'}\frac{\partial u_i}{\partial x_j} \tag{6a}$$

$$\mu_t = C_\mu \frac{\rho k^2}{\varepsilon} \tag{6b}$$

$$C_\mu = 0.033; \quad C_1 = 1.45; \quad C_2 = 1.9 \;; \sigma_k = 1; \quad \sigma_\varepsilon = 1.3 \tag{6c}$$

The effects of terrain roughness (or vegetation effects) are modelled by assigning a variation of velocity near the ground according to the logarithmic law:

$$\frac{u(z)}{u_*} = \frac{1}{\kappa}\ln\left(\frac{z}{z_0}\right) \tag{7}$$

where κ is the von Karman constant (0.41), z_0 is the roughness parameter (usually 0.03 to 0.25 times the physical vegetation height) and u_* is the friction velocity, which is computed as a function of the shear stress τ_w:

$$u_* = \sqrt{\frac{\tau_w}{\rho}} \tag{8}$$

The momentum transfer near the ground (shear stress) is thus computed as follows:

$$\tau_w = \rho\left[\frac{\kappa u_1}{\ln(z_1/z_0)}\right]^2 \tag{9}$$

where the subscript 1 indicates the value computed at the closest node to the ground.

Coriolis effects are neglected in this work, which, for characteristic lengths up to 20–30 kms is a reasonable assumption.

2.3. Grid generation

The application of CANYON for steep topography may pose convergence problems, arising from the higher degree of grid skewness that may be present. To avoid this, a numerical grid generation scheme was implemented (Lopes et al., 2001). This is based on the solution of a Poisson system that relates the Cartesian (x,y,z) and the computational (ξ,η, ζ) coordinates, as follows:

$$\begin{aligned} \xi_{xx} + \xi_{yy} + \xi_{zz} &= P_c + P_t \\ \eta_{xx} + \eta_{yy} + \eta_{zz} &= Q_c + Q_t \\ \zeta_{xx} + \zeta_{yy} + \zeta_{zz} &= S_c + S_t \end{aligned} \tag{10}$$

The right hand side terms are the so called control functions that allow the user to adjust the grid spacing and clustering near the ground boundary, and to control how the orthogonality conditions are transmitted to the interior domain (cf. Lopes et al., 2001, for details on the numerical method).

For the model NUATMOS, a simple algebraic grid generation, based on the application of expansion factors in the vertical direction, is performed. Due to their more general character, CANYON grids cannot be used in NUATMOS.

3. The graphical interface of WindStation

Since WindStation is implemented in the graphical environment of Microstation, the user may take benefit of all CAD tools for adding text labels and drawings, make dynamic rotations and zooms, or apply rendering options, for further working in the visualisation.

3.1. Grid generation

The module for grid generation reads terrain elevations from an ASCII file containing the x,y,z coordinates of the points located in a uniformly spaced rectangular grid. The user may then override the recommended height for the domain, grid spacing near the ground and number of vertical layers. The corresponding Dialog Box is displayed in Fig. 1.

3.2. Input data

The main input data for both wind models are the wind speed and direction readings at the meteo stations

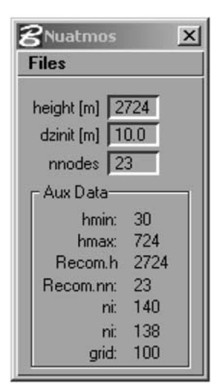

Fig. 1. Dialog Box for the input of grid characteristics.

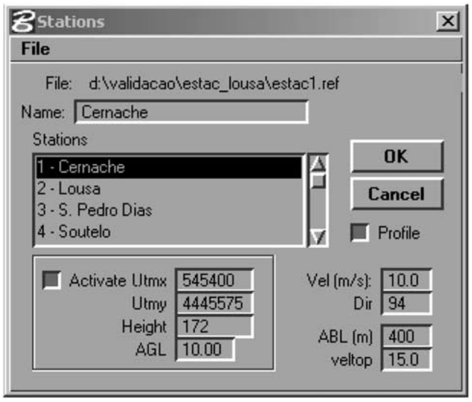

Fig. 2. Dialog Box for definition of the meteo stations data.

location. The definition of the different stations available and their location is performed in the Dialog Box presented in Fig. 2.

If the user wants to consider, as input, not only the station reading, but also a velocity profile, an estimation of the boundary layer height as well as the corresponding velocity should be input as well. The code then calculates the boundary layer profile according to a power law, as follows:

$$\frac{v}{v_\infty} = \left(\frac{z}{\delta}\right)^{1/\alpha} \tag{11}$$

where v is the velocity corresponding to the height z and v_∞ is the wind speed at the boundary layer height δ. The exponent α is computed according to the input data.

3.3. Control parameters

For the model CANYON, the user specifies the terrain roughness (which is assumed as constant for the overall domain, in the present implementation), maximum number of iterations and maximum residual for the equations as convergence criteria. The input file, obtained from the grid generation module, as well as the file for storing the calculation results, are specified in the corresponding fields (cf. Fig. 3).

For the NUATMOS model, the main input parameters are the atmospheric stability parameter (alpha), the converge parameter and the maximum number of iterations (cf. Fig. 4).

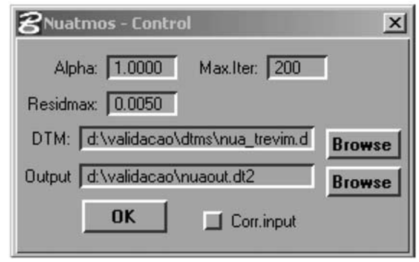

Fig. 4. Dialog Box for NUATMOS input parameters.

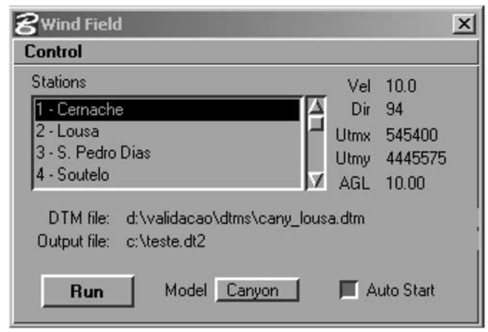

Fig. 5. Dialog Box for launching the wind simulation software.

The Dialog Box represented in Fig. 5 allows the user to review the input data, choose the wind model and launch the calculation process.

3.4. Post-processing

The Dialog Box shown in Fig. 6 allows the user to display the terrain map, coloured according to the local terrain height.

For displaying the wind field, a vectorial representation is employed. The user may control the colouring scheme, the spatial density of vectors, as well as scaling factors, among other features. The Dialog Box for vectors representation may be seen in Fig. 7.

Another method for analysing the calculation results is to perform a dynamical probing of the domain. Using the tools available in the Dialog Box shown in Fig. 8, the user may interrogate any spatial location and get the

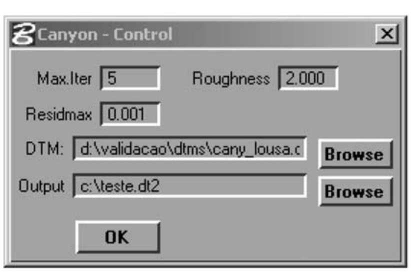

Fig. 3. Dialog Box for CANYON input parameters.

Fig. 6. Dialog Box for representation of the topography.

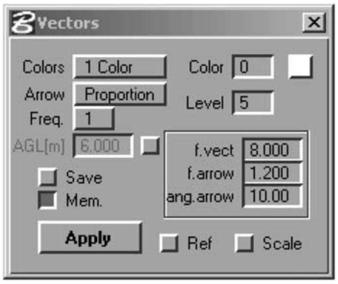

Fig. 7. Dialog Box for representation of wind vectors.

local UTM coordinates and terrain height, wind speed and direction (cf. Fig. 9). At the selected location, the code may generate the vertical profile for wind speed and direction, and store the respective values in an ASCII file. The model output at pre-defined locations may be displayed by selecting the desired location in the corresponding field (cf. item Stations in the Dialog Box of Fig. 8). This is very useful, for example, to compare the computed wind values with the values measured by the meteo stations.

4. Test case—the Askervein experiment

The Askervein experiment consisted of a multinational research project for the characterisation of wind flow over smooth topography. The experiments were carried out in Askervein, an isolated hill of 116 m height located near the South Uist coast, in Scotland. Data, collected in 1982 and 1983, are reported by Taylor and Teunissen (1987). The hill shape is slightly elliptical in planform with a major axis of approximately 2 km and a minor axis of approximately 1 km. The hill shape may be appreciated in Fig. 10, where the 3 m contour lines are represented.

The hill shape along lines A and B is depicted in Figs. 11 and 12, respectively. The x-axis runs from south to north, for line A and from west to east, for line B. According to Taylor and Teunissen (1987), the hill surface is relatively uniform, covered with short, coarse grass, low heather and flat, exposed rock. The same authors refer a roughness parameter of 0.03 m as a good value for describing this type of terrain.

The program consisted in measuring wind speed, direction and turbulence intensity along lines A, B and

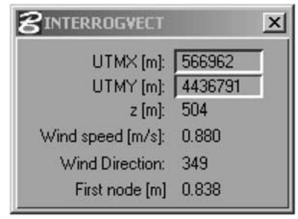

Fig. 9. Output for the dynamic field probing.

AA (cf. Fig.10), employing 10–50 m height meteo masts. A reference station placed 3 km SSW of the hill provided data for the incident undisturbed boundary layer profile. The reported simulations are for an incident wind direction of 210° to the North (approx. SW).

For the present simulations, incident wind data was generated running a 1D version of CANYON. The velocity boundary layer is presented in Fig. 13. In this picture, the local velocity is non-dimensionalised with the velocity measured at the reference station. As may be appreciated, quite a good agreement was obtained between the numerical and the experimental results. This wind profile was adopted for the simulations with the NUATMOS model as well.

Calculations were performed in a 60 m square grid, with 20 nodes in the vertical direction. The graphic depicted in Fig. 14 represents the variation of wind speed-up at a height of 10 m above ground level, along line A. Wind speed-up is defined as follows:

$$\Delta S = \frac{v(z)}{v_{rs}(z)} - 1 \qquad (12)$$

where v is the local velocity, v_{rs} is the velocity at the reference station and z is the distance above ground level. The x-axis represents the distance to the location HT (hill top, cf. Fig. 10). Analysis of this graph shows that, up to the summit of the hill, the agreement for both NUATMOS and CANYON, with the experimental results, is very good. On the other hand, on the downstream side, NUATMOS shows remarkable differences. This behaviour is not surprising, due to the kinematic character of this model. If the hill was perfectly symmetric, the results given by NUATMOS would be similar on the upstream and downstream side of the hill. Results along line B, which goes along the summit of the hill, in a direction approximately perpendicular to the incident flow direc-

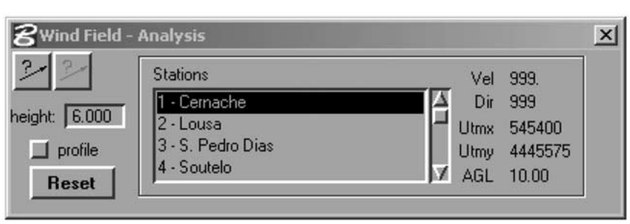

Fig. 8. Dialog Box for dynamic field probing.

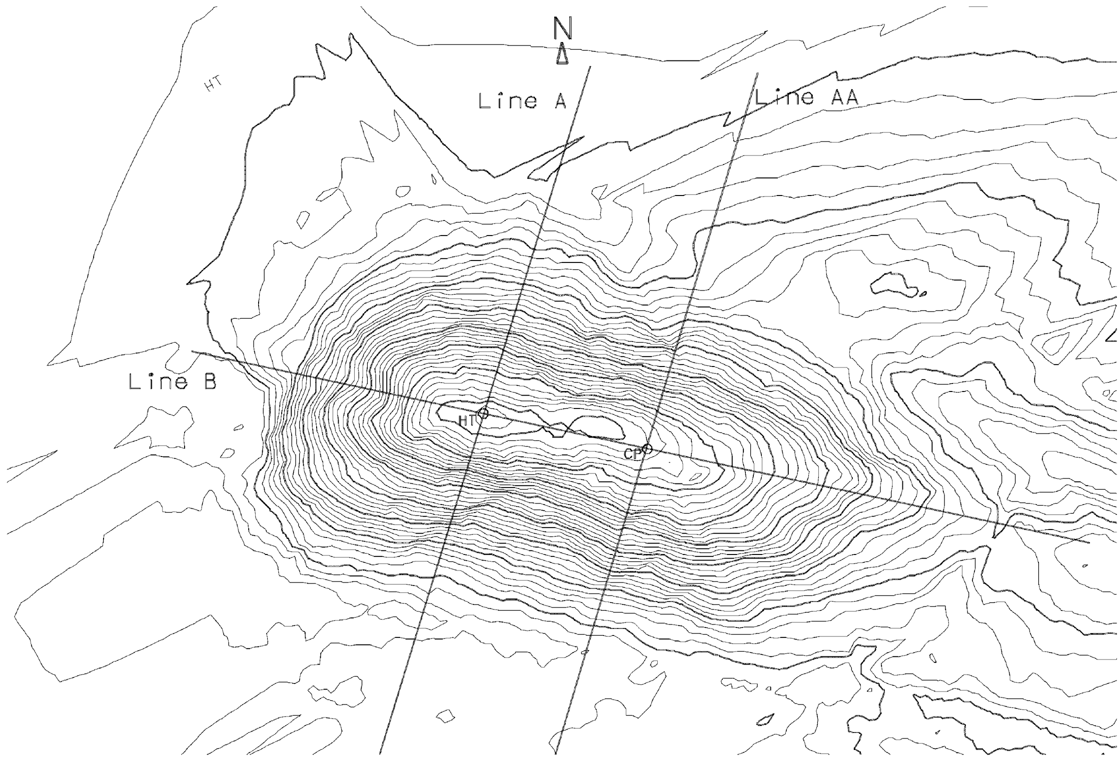

Fig. 10. Askervein Hill: 3 m contour levels.

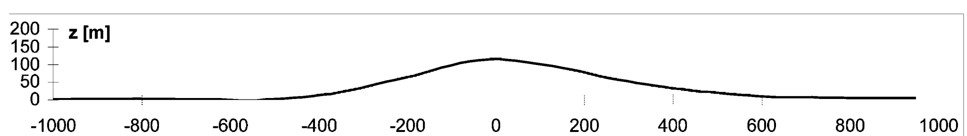

Fig. 11. Askervein Hill profile along line A.

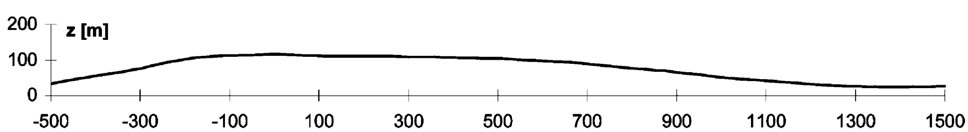

Fig. 12. Askervein Hill profile along line B.

tion, are presented in Fig. 15. In this case, the agreement is satisfactory for both models.

Fig. 16 depicts the angle between the local wind direction and the incident flow direction, along line A. Taylor and Teunissen (1987) consider the measurement at HT (hill top, x=0) to be suspect. Once again, CANYON shows a good agreement with the experimental values. In this case, NUATMOS performs quite poorly.

The vectorial representation of the simulated wind field may be appreciated in Figs. 17 and 18 for NUATMOS and CANYON, respectively. It is well evident in these figures that, downstream of the hill, the linear model NUATMOS recovers in a much higher degree the approaching wind speed.

5. Test case—mountainous region in Portugal

The Askervein case presented previously constitutes a good reference for models testing, due to the considerable amount and quality of the available data and the "almost ideal" conditions: an isolated hill with uniform roughness cover and a well developed incident boundary layer profile. In general, such input data is not available when one intends to make computations for complex topography. The measurements available are, normally, readings at meteo stations, and no information is available concerning the boundary layer profiles, thermal stratification or surface roughness. In general, these parameters must be guessed, leading to a much poorer accu-

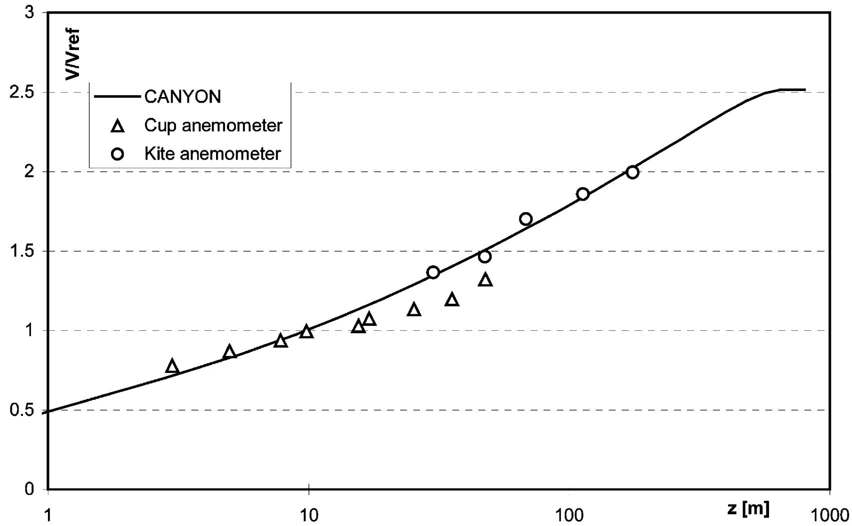

Fig. 13. Incident boundary layer profile.

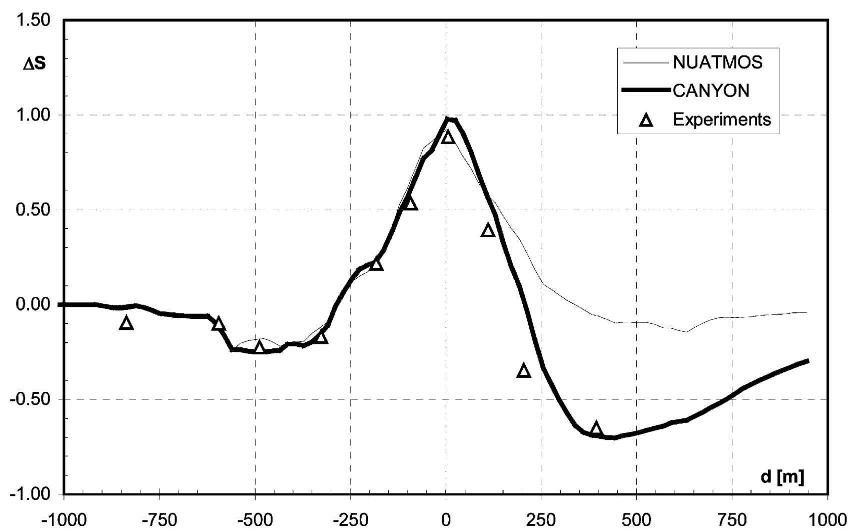

Fig. 14. Wind speed-up along line A.

racy. In the present section, some results will be presented for situations were input data is sparse. This is the case at a mountainous region in Central Portugal, where the vegetation is spatially diverse and only a few meteo stations are available. Temporal steadiness in terms of wind direction and speed was used as a criterion for choosing sample data.

5.1. Characteristics of the different runs

The results obtained with both CANYON and NUATMOS will be compared with the data measured by the meteo stations. The following types of simulations were considered:

For NUATMOS:

Simulations A: in this case, all the meteo stations serve as input data for the model. No correction is applied to the input data (cf. Eq.1). The analysis compares the input data with the data obtained at each station, after the simulation. These simulations intend to quantify how the model predictions deviate from the initial boundary conditions. If input data correction were applied, the indices would be 100 (cf. section 5.2).

Simulations B: the computed values at each meteo station are obtained running the model using the remaining stations as input data, with no input correction.

Simulations C: similar to simulations B, except that Eq. (1) is employed for correction of the input data.

For CANYON:

Simulations were made taking as input data the values measured at the meteo station of Soutelo, in the region of Poiares.

For the region of Trevim, the two situations considered (A and B) correspond to different grid cell sizes.

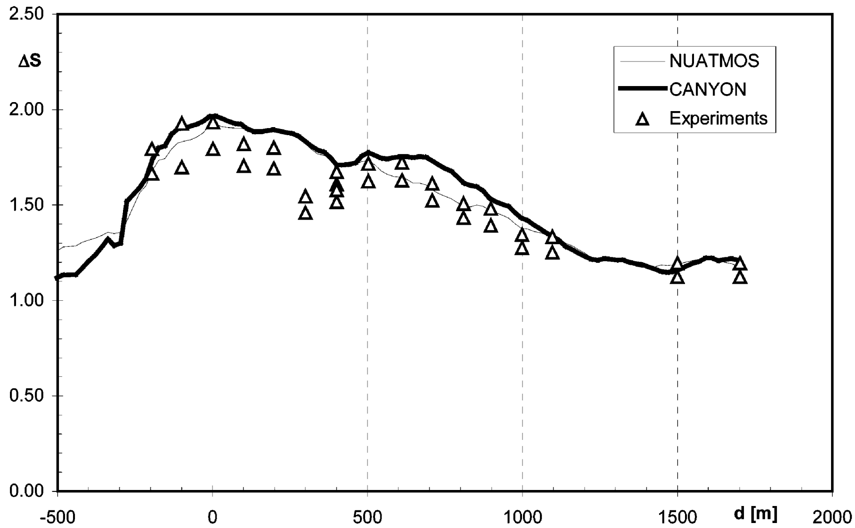

Fig. 15. Wind speed-up along line B.

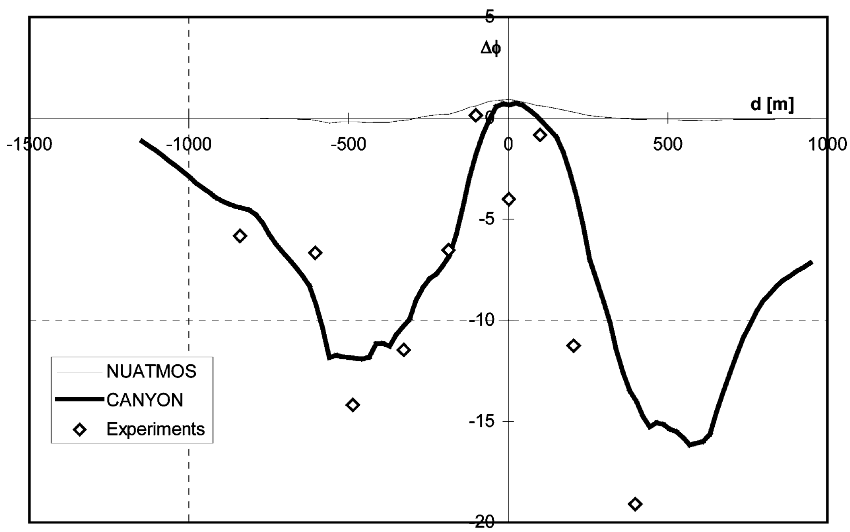

Fig. 16. Flow angle along line A.

5.2. Performance indices

Comparison between computed and observed data was done through the following indices:

Index for wind speed: this index was derived with recourse to an exponential relation, to allow the index to tend asymptotically to zero as the deviation between measured and simulated data increases. The mismatch between these two variables was quantified by their ratio:

$$I_v = 100.e^{\left[-0.692\left(\frac{v_1}{v_2}-1\right)\right]} \quad (13)$$

where v_1 and v_2 are the observed and the simulated wind velocities, or vice-versa, with $v_1 > v_2$. The factor 0.692 was adopted to force the index to assume the value 50 when the ratio between both velocities is 2 (or 1/2). The graphical representation of the dependence of the index with the velocity ratio is depicted in Fig. 19.

Index for direction:

The formula adopted assumes a sinusoidal variation of the index with the angle between the computed and the observed wind direction, as follows:

$$I_d = 50 + 50.\cos(\Delta\theta) \quad (14)$$

where I_d is the direction index and delta theta is the angle between the simulated and the observed wind direction. Fig. 20 represents the relation between the index and delta theta. In the ideal situation the index value is 100, while in the worst case, i.e., when the angle between the two velocity directions is 180°, the index value is zero.

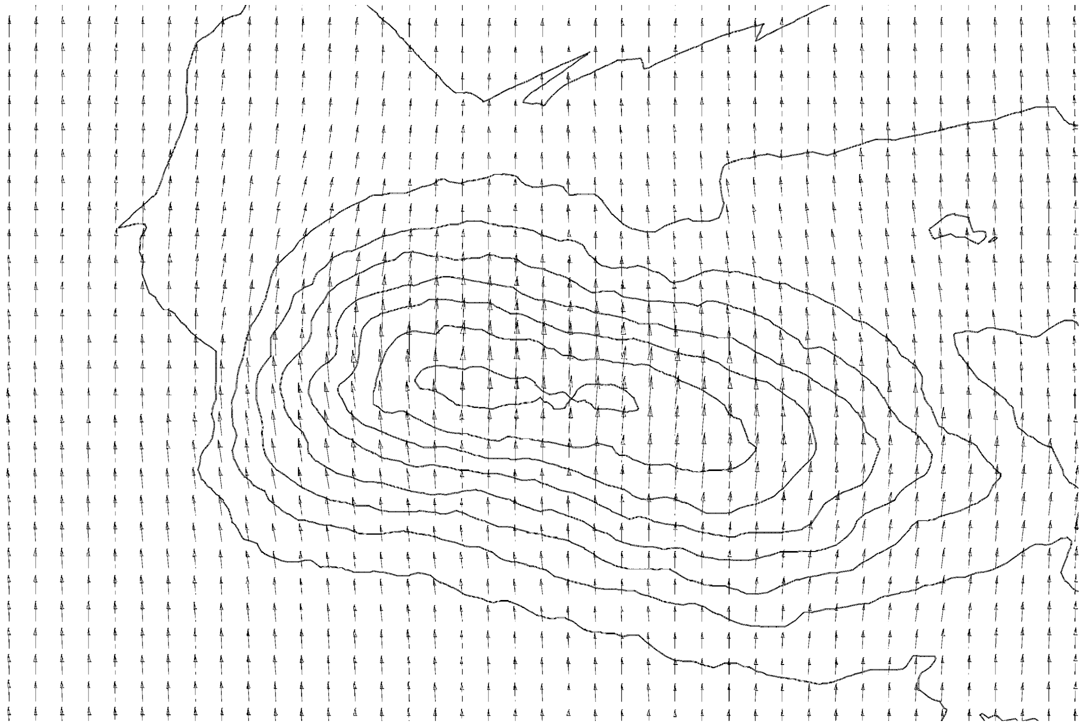

Fig. 17. Wind field at 10 m obtained with NUATMOS.

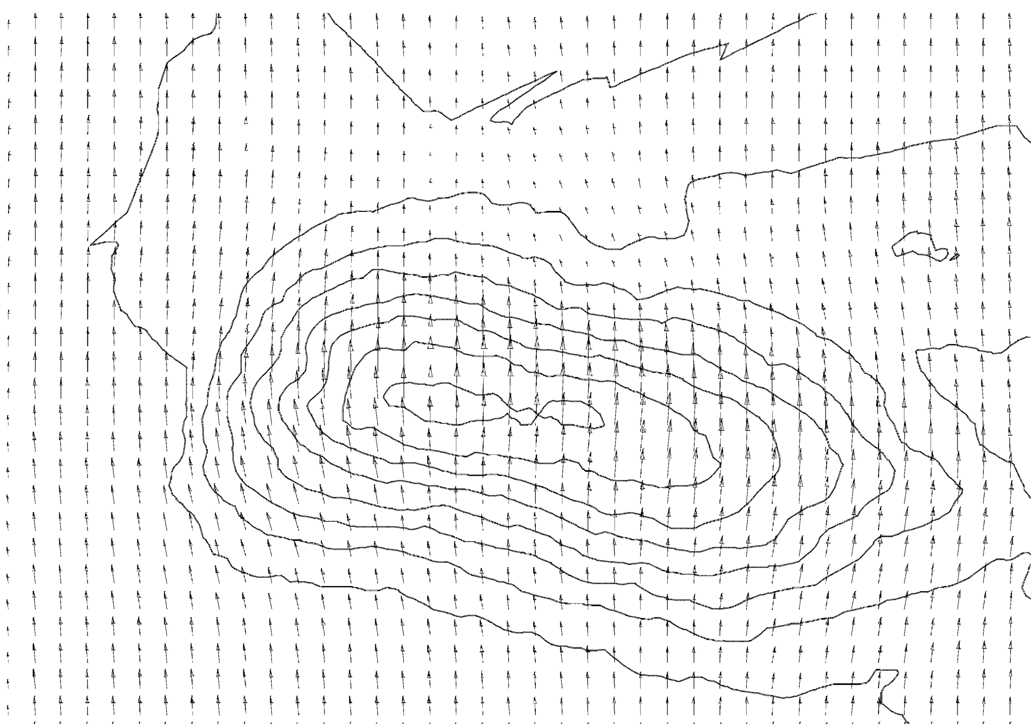

Fig. 18. Wind field at 10 m obtained with CANYON.

5.3. Simulations for the region of Poiares

The Poiares study region is located in central Portugal, approximately 30 km away from the city of Coimbra (cf. Fig. 21). In terms of topography, this region is mostly flat. Fig. 22 depicts the calculation domain, which is 15×13.5 km². The meteo stations are identified in the figure. The mast of Soutelo was located in the top of a

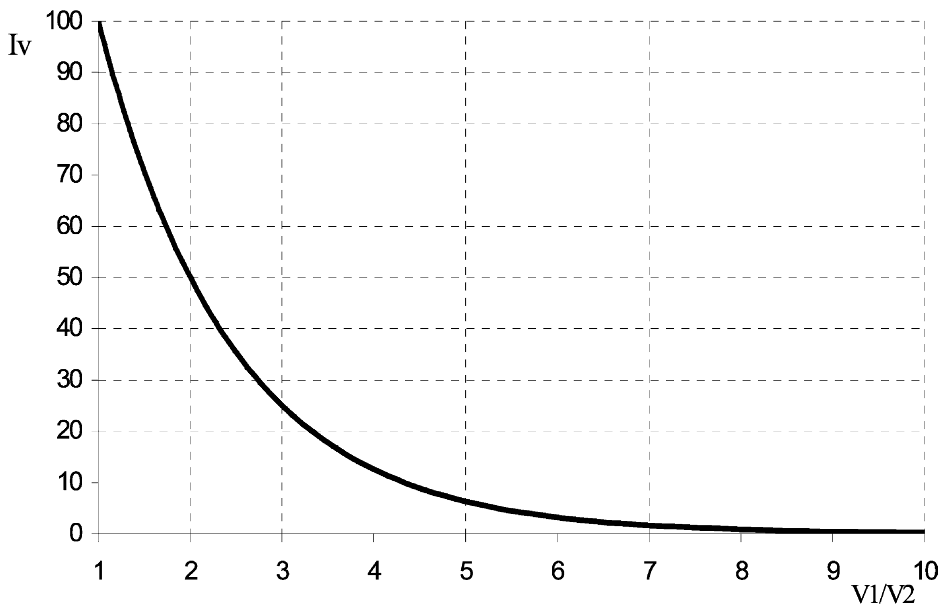

Fig. 19. Relationship between velocity mismatch and velocity index.

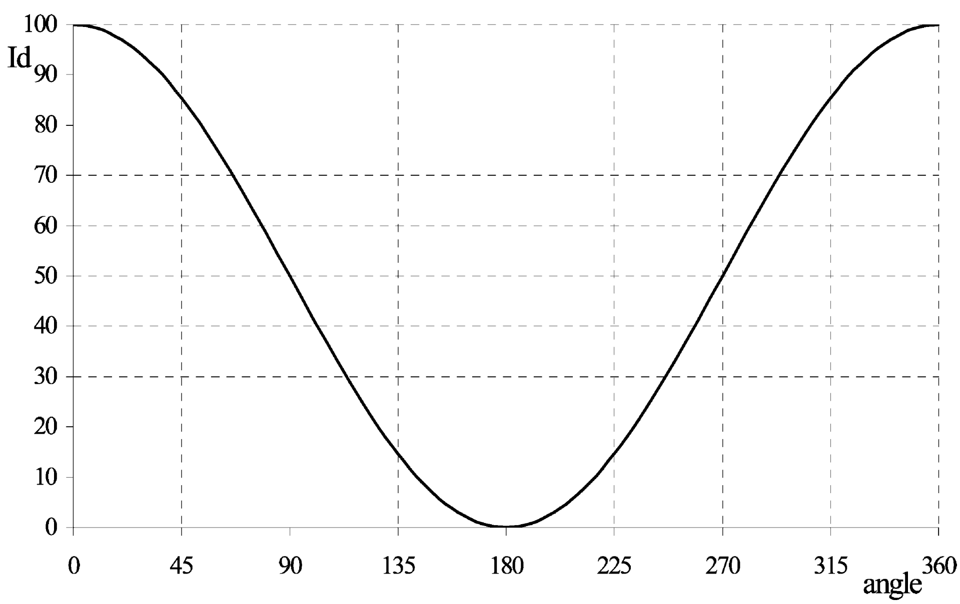

Fig. 20. Relationship between direction mismatch and direction index.

watchtower. S. Pedro Dias station is a 10 m mast located at a hill top. The mast of Lousã is located in a small flat region, which serves as a local aerodrome. This location is surrounded by trees which, as will be seen later, affected in a considerable manner wind speed data. The three stations considered in this region were instrumented with an anemometer and a direction vane. Dataloggers acquired data every second and stored the average values every 10 minutes. For the simulations, hourly averages were considered. Some care was taken in selecting periods of as steady wind speed and direction as possible. Some data concerning these meteo stations are in Table 1.

Data employed for the simulations were acquired in the period of March 3–October 7, 2000. A total of 44 different hourly averages were chosen. For the computer runs, a grid of 140×138×15 nodes, with a cell size of 100×100 m^2, with the first grid node 1 m from the ground, was employed for NUATMOS. For CANYON, the grid had 97×93×22 nodes, with 150×150 m^2 for cell size and the first grid node was placed 2m from the ground. Due to the lack of vegetation cover maps, a uniform roughness of 2 m was considered for the entire domain.

Table 2 summarises the values obtained for the indices averaged for the three stations. The values presented in *italic* are the standard deviation for each index. One may

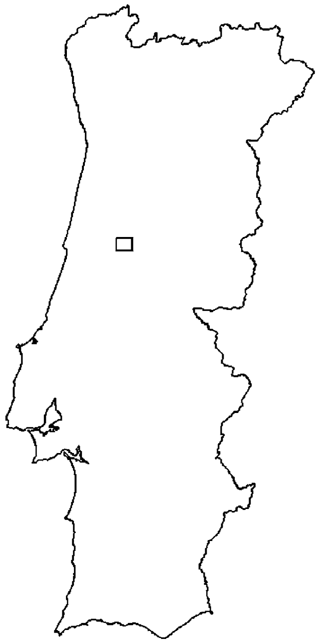

Fig. 21. Approximate location of the region of Poiares, in Portugal.

observe that the direction indices are very good. In terms of velocity magnitude, raw data indicated that the wind values computed at Lousã are quite low, due to the shielding effect of the trees surrounding the area. This is a local effect that was not taken into account in the simulation, and thus the indices obtained in this location are very low. This may be observed in Table 3, were the average index computed for each station is presented.

The agreement between simulated and measured values is, in general, for the remaining stations, not very satisfactory. One may observe that the standard deviation of the indices is quite high, indicating a considerable spread of the data. Raw data showed cases where the agreement is excellent, while, for other cases, the agreement is very low. Apparently, the correction of input data for NUATMOS (situation C) does not improve the agreement. CANYON seems to perform better than NUATMOS, although the differences are not very significant.

Table 4 presents the average indices for each calculation method, without taking into account Lousã station. This leads to indices values that are already quite acceptable.

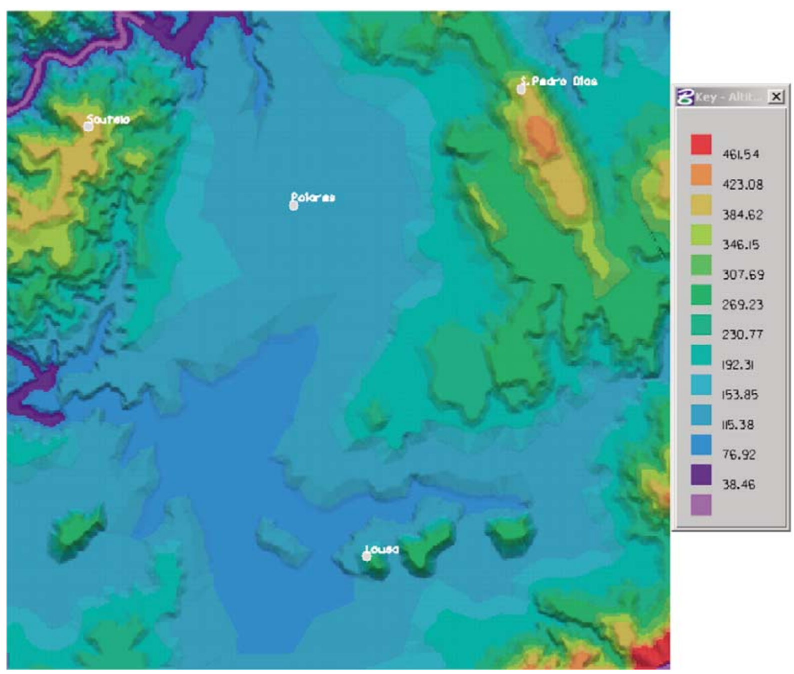

Fig. 22. Digital terrain model of the Poiares region and location of the meteo masts. North is at top. Domain is 15×13.5 km^2.

Table 1
Data for the meteo stations located at Poiares region [m]

Station	Utm x	Utm y	Altitude	Height
Soutelo	558957	4453106	432	18.6
SP.Dias	567916	4453884	358	10
Lousã	564721	4444273	201	10

Table 2
Average indices for Poiares region. (average/*rms*)

	NUA.A	NUA.B	NUA.C	CAN.A
I_v	61/*23*	54/*37*	49/*36*	56/*32*
I_d	99/*2*	83/*32*	89/*7*	90/*22*

Table 3
Average indices computed at each station (Soutelo/SPDias/Lousã)

	NUA.A	NUA.B	NUA.C	CAN.A
I_v	80.0/61.0/43.0	81.7/70.2/10.0	66.0/75.8/4.4	75.4/76.6/15.1
I_d	99.9/98.9/97.7	90.4/77.8/79.8	86.2/86.2/93.3	90.2/99.6/80.4

Table 4
Average indices for Poiares region, excluding Lousã mast in the computation of the index

	NUA.A	NUA.B	NUA.C	CAN.A
I_v	70	76	49	76
I_d	99	84	88	95

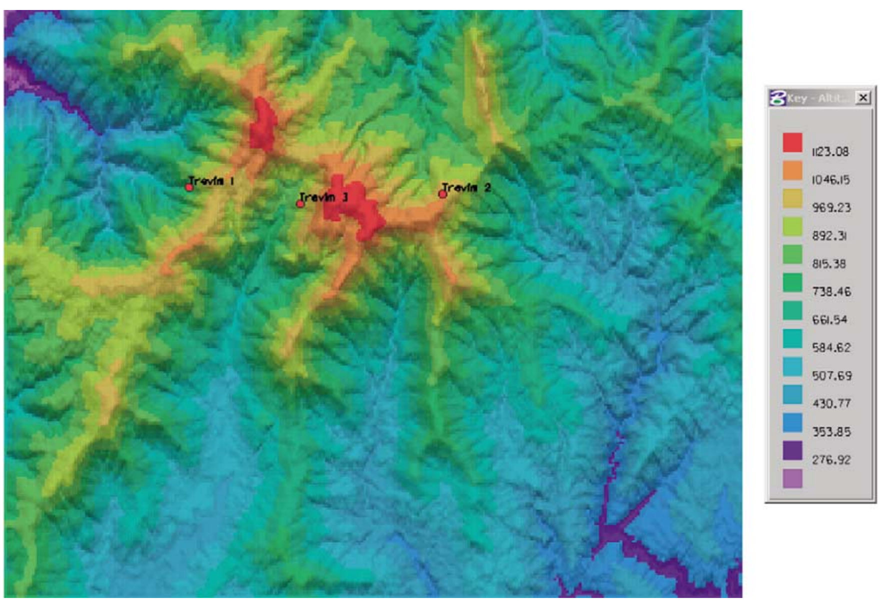

Fig. 23. Digital terrain model of the Trevim region and location of the meteo masts. Domain is *15×13.5 km²*.

5.4. Simulations for the region of Trevim

In terms of topography, the region of Trevim is considerably steeper than the region of Poiares. Geographically, it is located approximately 15 km South-East of Poiares region. Figs. 23 and 24 depicts the topography, as well as the location of the three meteo masts employed for the wind measurements. The domain of calculation is 14.5×11.5 km^2. For these runs, portable masts were installed at mid-slopes or valleys, in order to check how the models behave for these type of situations. The masts' height (6 m) was, nevertheless, somewhat small. In fact, vegetation height at some locations surrounding the masts was close to 2 m, with some isolated trees. It is believed that this affected the measured data.

The data used for the simulations were acquired in the period March 3–14, 2000. A total of 44 different hourly

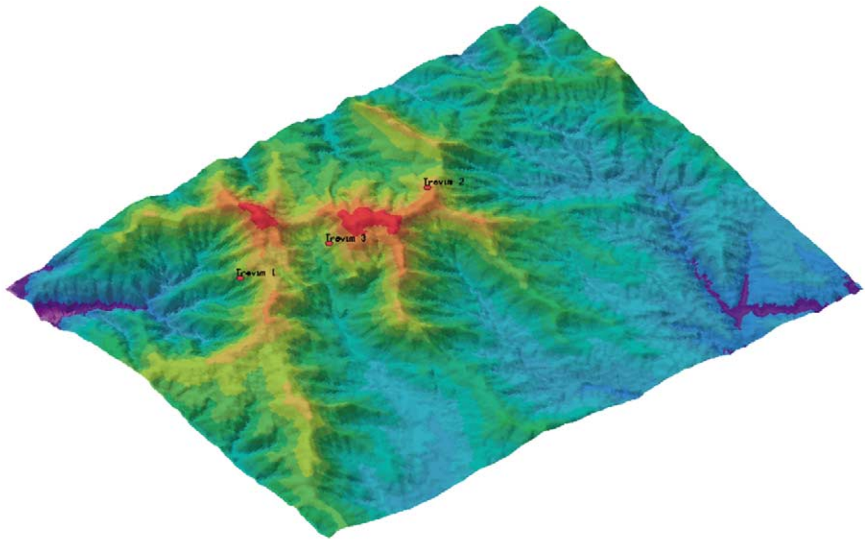

Fig. 24. Digital terrain model of the Trevim region and location of the meteo masts. Perspective view.

averages were used. For NUATMOS, a grid with 105×77×15 nodes and a cell size of 100×100 m^2 was employed. The first node was placed at a distance of 1 m from the ground. For CANYON, the grid was 105×77×22, with 100×100 m^2 and 40×40 m^2 for cell size for situation A and B respectively, and the first grid node was placed 2 m from the ground. A uniform roughness of 2 m was considered for the entire domain. Some data concerning the meteo stations is presented in Table 5.

Table 6 shows the average indices as well as their standard deviation values for the different runs. For NUA.A, where all the stations are used as source for input data, the indices present a quite low value. This is due to the fact that the topography is so steep that the initial values suffer a big adjustment when the code attempts to reach a divergence free flow field. Changing the type of NUATMOS input (situations B and C) shows some improvements for some stations, while, for others, the results are worse. It is, thus, difficult to draw definitive conclusions about which method is the best. Analysis of the raw data revealed that there are situations where the agreement is very good, while for others the agreement is quite poor.

The results obtained for CANYON are also not encouraging. It may be noted that the results for Station 1 in particular are not good. In fact, the experimental readings at this station in terms of wind speed were suspiciously low most of the time. Table 7 presents the average index for each station separately.

Some runs for more refined grids were made with CANYON, to check if some improvement could be obtained using a 40×40 m^2 cell size (CAN.B). Although this led to some differences in the velocity field, the average value of the indices did not improve significantly.

The velocity fields obtained by NUATMOS and CAN-

Table 5
Data for the Trevim meteo stations [m]

Station	Utm x	Utm y	Altitude	Height
Station 1	568708	4437140	935	6
Station 2	573715	4437010	999	6
Station 3	570895	4436819	993	6

Table 6
Average indices and corresponding standard deviation

	NUA.A	NUA.B	NUA. C	CAN. A	CAN.B
I_v	57/*30*	47/*31*	60/*32*	41/*36*	41/*33*
I_d	77/*27*	63/*32*	55/*37*	54/*38*	63/*33*

Table 7
Indices computed at each station (Location 1/Location 2/Location 3)

	NUA.A	NUA.B	NUA.C	CAN.A	CAN.B
I_v	40/67/65	37/49/54	60/37/50	13/71/39	27/56/41
I_d	80/89 62	75/55/59	54/41/70	45/70/45	52/81/54

YON, for situation A, are represented in Figs. 25 and 26, respectively. It is very interesting to note the similarity of both computations in the upstream side of the hills, while, on the other hand, completely different results are obtained in the downstream side, with recirculation regions clearly predicted by CANYON.

The effect of local grid refinement at the location of Station 3 may be observed in Fig. 27. It is clear that the refinement of the grid may lead to differences in wind speed and direction.

6. Conclusions

A code aimed at the simulation of atmospheric flows over complex terrain was presented. Its graphical implementation proved to be very advantageous in terms of data input and analysis of the results. The applications presented here light up the strengths and weaknesses of this type of simulation. The implementation of the physical equations and models for fluid flow were able to give quite accurate predictions provided accurate boundary conditions were supplied, as in the case of the Askervein hill. For situations where terrain roughness is not accurately described, local terrain features are not sufficiently detailed for being modelled, and approaching boundary layer profiles are not known, comparison of measured data and simulated data is not expected to give impressive results. Further to these factors, the wind variability in time is another source of error that may have played an important role for the simulations of Poiares and Trevim. The fact that one is evaluating a model performance at a location some kilometres away from the place where input data was taken, means that the temporal displacement may pay an important role if one thinks of wind variability. Nevertheless, results obtained for the regions of Poiares were quite acceptable for two locations.

Rather than trying to simulate accurate values for both wind speed and direction, which is very difficult in real terrain topography, due to the reasons pointed previously, this type of approach is believed to be more useful for producing maps of wind behaviour and comparing the relative "performance" of different locations. Within this frame, numerical tools such as the one

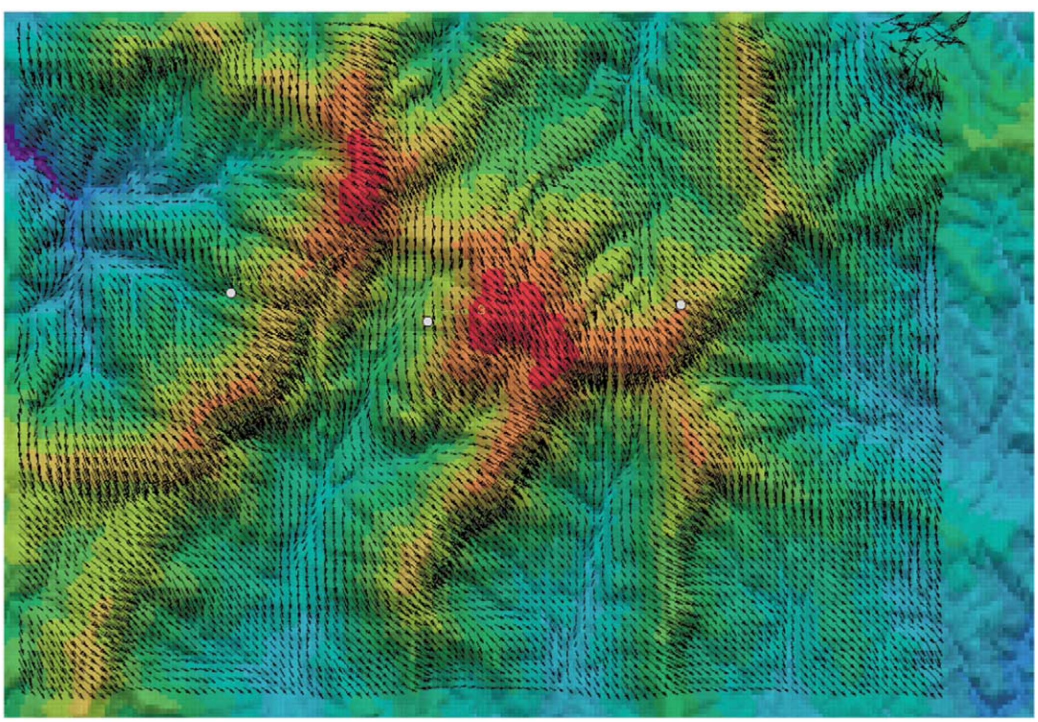

Fig. 25. Velocity field obtained by NUATMOS-run #13, situation A.

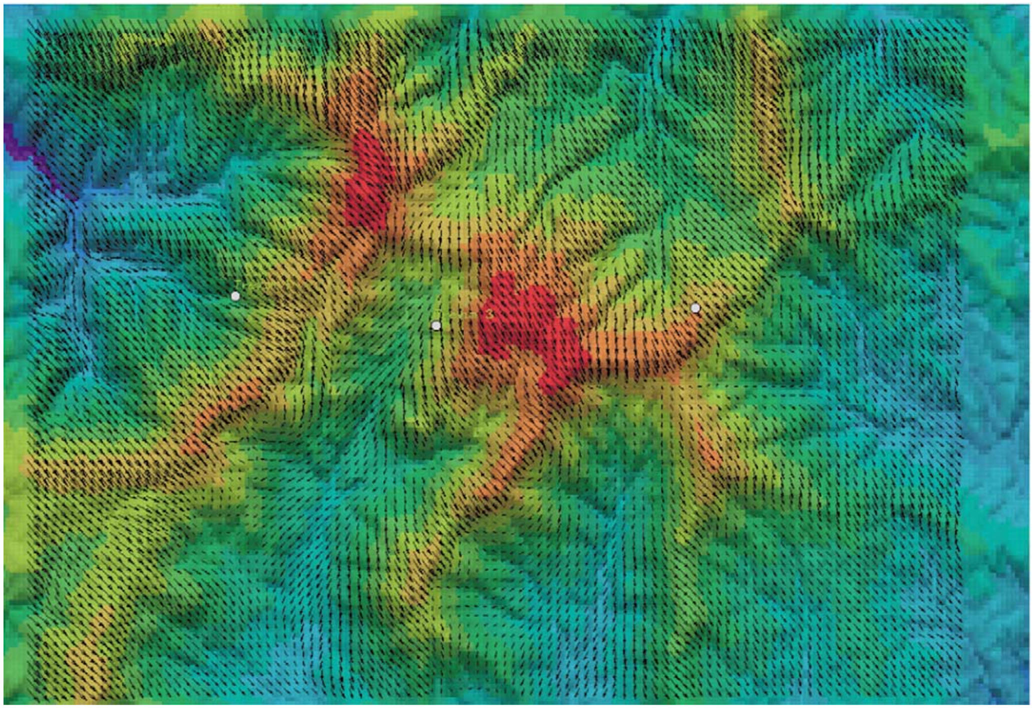

Fig. 26. Velocity field obtained by CANYON-run #13, situation A.

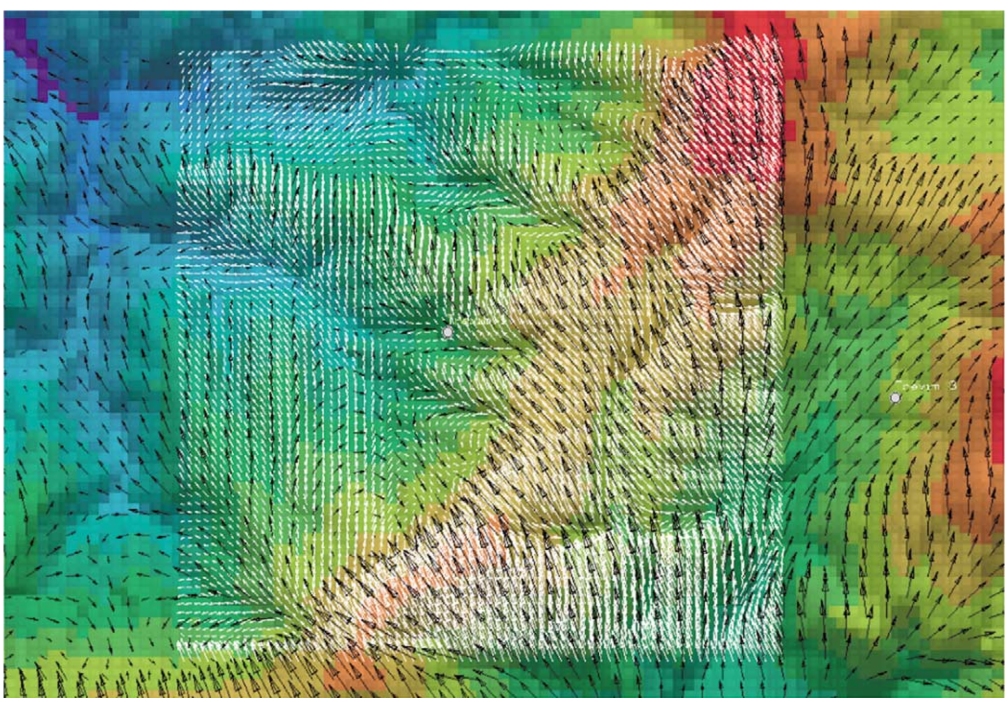

Fig. 27. Comparison between the velocity field obtained with a *100 m* cell size (black vectors) and the velocity field obtained with a *40 m* cell size (white vectors).

presented here, may be valuable aids for making the assessment of the relative characteristics of terrain locations for applications such as wind turbine siting, smoke dispersion or forest fire behaviour.

Acknowledgements

The development of the models and graphical interface was carried out under the scope of the research project entitled “An Integrated System for the Prediction of the Risk and Behavior of Forest Fires”, Project PRAXIS XXI 3/3.1/CEG/2639/95, funded by JNICT *Junta Nacional de Investigação Científica e Tecnológica*, Portugal.

Experimental data and simulations for complex topography were made under the scope of the project “INFLAME—Fire Behaviour Prediction—Modelling and Testing”, funded by the European Commission, Contract ENV4-CT98-0700.

The author is grateful to Prof. Domingos Xavier Viegas for his support and to Eng. António José Silva for is co-operation gathering experimental data.

References

Alm, L.K., Nygaard, T.A., 1995. Flow Over Complex Terrain Estimated by a General Purpose Navier-Stokes Solver. Modelling, Identification and Control 16 (3), 169–176.

Flassak, T., Moussiopoulos, N., 1988. Direct solution of the Helmholtz equation using Fourier Analysis on scalar and vector computers. Environmental Software 3, 12–16.

Jackson, P.S., Hunt, J.C.R., 1975. Turbulent Flow Over a Low Hill. Quarterly Journal of the Royal Meteorological Society 101, 929–955.

Launder, B.E., Spalding, D.B., 1974. The Numerical Computation of Turbulent Flows. Computer Methods in Applied Mechanics and Engineering 3, 269–289.

Lopes, A.M.G., Sousa, A.C.M. and Viegas, D.X., 2001, Grid3D—Um Código para a Geração Numérica de Malhas Generalizadas Estruturadas. Ingenium, in press (in Portuguese).

Lopes, A.M.G., Sousa, A.C.M., Viegas, D.X., 1995. Numerical Simulation of Turbulent Flow and Fire Propagation in Complex Terrain. Numerical Heat Transfer Part A (27), 229–253.

Patankar, S.V., 1980. Numerical Heat Transfer and Fluid Flow. Hemisphere Publishing Corporation, Washington, DC.

Raithby, G.D., Stubley, G.D., 1987. The Askervein Hill Porject: A Finite Control Volume Prediction of Three-Dimensional Flows over the Hill. Boundary-Layer Meteorology 39, 247–267.

Ross, D.G., Smith, I.N., Manins, P.C., Fox, D.G., 1988. Diagnostic wind field modeling for complex terrain: Model development and testing. Journal of Applied Meteorology 27, 785–796.

Szulényiová, A., 1992. Diagnostic Wind Field Model in a Complex Terrain, Contributions of the Geophysical Institute of the Sloval Academy of Sciences. Series of Meteorology 12, 85–98.

Taylor, P.A., Teunissen, H.W., 1987. The Askervein Hill Project: Overview and Background Data. Boundary Layer Meteorology 39, 15–39.

Taylor, P.A., Walmsley, J.L., Salmon, J.R., 1983. A Simple Model of Neutrally Stratified Boundary-Layer Flow Over Real Terrain Incorporating Wavenumber-Dependent Scaling. Boundary Layer Meteorology 26, 169–189.

Uchida, T., Ohya, Y., 1999. Numerical Simulation of Atmospheric Flow over Complex Terrain. Journal of Wind Engineering and Industrial Aerodynamics 81, 283–293.

Van Doormaal, J.P., Raithby, G.D., 1984. Enhancements of the Simple Method for Predicting Incompressible Fluid Flows. Numerical Heat Transfer 7, 147–163.